4f4f Wiki Article of Project Q

Anja Appenzeller Florian Bruder Marcel Lukanowski Nina Rauwolf
Dominik Steinmetz

June 2024

1 Introductory remarks

The aim of this article is to give a brief overview over the topic of quantum chemical calculations on lanthanide systems. First, a small introduction is given on the basics of quantum chemical calculations. Afterwards, different calculations on lanthanide systems are discussed. More information on how to actually perform calculations with TURBOMOLE can be found in the manual.[1]

2 Basics of Quantum Chemistry

2.1 Schrödinger equation

The central equation in most of quantum chemistry is the time independent Schrödinger equation[2],[3]

$$\hat{H}\Psi = E\Psi\,, \tag{1}$$

where the Hamilton operator $\hat{H}$ collects operators of all relevant energy contributions of the system. The wave function Ψ describes the state of said system with the respective energy E. For most systems, several distinct pairs of Ψ and E are valid solutions to the Schrödinger equation with a given Hamilton operator. In the special case of the electronic Schrödinger equation in the context of molecules in quantum chemistry, the solution with the lowest energy E gives the electronic ground state. All other solutions represent excited electronic states respectively.

2.2 Molecules within the Born–Oppenheimer approximation

When applying the Schrödinger equation to molecular systems, the Born–Oppenheimer (BO) approximation[4] is employed in the vast majority of cases. Here, the atomic nuclei are described as being fixed in space and are usually assumed to be point charges. For a given arrangement of nuclei, only the electrons are treated in a quantum mechanical manner. The use of the Born–Oppenheimer approximation can be justified by examining the time scales of the movement of nuclei and electrons. Electrons are much lighter than atomic nuclei (a proton is approximately 1800 times heavier than an electron[5]). Thus, nuclei typically move much slower than electrons and can therefore be treated as stationary.

Now the electronic Hamilton operator can be set up by collecting different energy contributions of kinetic energies and potential energies. A molecular system consists of positively charged nuclei and negatively charged electrons. The kinetic energy of the nuclei is omitted withing the BO approximation since they are stationary. The kinetic energy of the electrons is given by the respective operator $\hat{T}_e$. Potential energy contributions arise from the Coulomb interaction of the charged particles, the two repulsive interactions of nuclei–nuclei and electrons–electrons, $\hat{V}_{nn}$ and $\hat{V}_{ee}$, and the attractive interaction of nuclei–electrons $\hat{T}_{ne}$. The full Hamilton operator is thus given as

$$\hat{H} = \hat{T}_e + \hat{V}_{ne} + \hat{V}_{ee} + \hat{V}_{nn}\,. \tag{2}$$

The Coulomb interaction between nuclei $\hat{V}_{nn}$ is just a constant value within the BO approximation and is therefore sometimes omitted in the electronic Hamilton operator and added to the total energy later.

2.3 Hartree–Fock theory

In the previous section an expression for the Hamilton operator was established. We will now look at one of several approaches to construct the electronic wavefunction Ψ.

The electronic wave function Ψ describes all N electrons contained in the system, meaning it is dependent on all electronic coordinates:

$$\Psi(\mathbf{x}_1, \mathbf{x}_2, \ldots, \mathbf{x}_N) \tag{3}$$

It is convenient to construct Ψ by using N one-particle wave functions $\phi_i(\mathbf{x})$ that each only depend on one electronic spin coordinate. These one-particle wave functions are know as molecular orbitals (MOs). A naive approach to construct the total wave function would be to use a simple product of molecular orbitals.

$$\Psi(\mathbf{x}_1, \mathbf{x}_2, \ldots, \mathbf{x}_N) = \phi_1(\mathbf{x}_1) \cdot \phi_2(\mathbf{x}_2) \cdot \cdots \cdot \phi_N(\mathbf{x}_N) \tag{4}$$

Here, electron 1 would be located in MO 1, electron 2 in MO 2 and so on. This approach is known as a Hartree-product and is not applicable to electrons. Electrons are fermions and therefore need to obey the Pauli exclusion principle. This means that the wave function needs to undergo a change in sign when interchanging any two electronic coordinates, e.g.

$$\Psi(\mathbf{x}_1, \mathbf{x}_2, \mathbf{x}_3, \mathbf{x}_4, \ldots, \mathbf{x}_N) = -\Psi(\mathbf{x}_4, \mathbf{x}_2, \mathbf{x}_3, \mathbf{x}_1, \ldots, \mathbf{x}_N)\,. \tag{5}$$

It can clearly be seen that the wave function in eq. (4) does not meet this requirement. The required change in sign can be obtained by the use of a Slater Determinant[6]

$$\Psi_{SD} = \frac{1}{\sqrt{N!}} \begin{vmatrix} \phi_1(\mathbf{x}_1) & \phi_2(\mathbf{x}_1) & \cdots & \phi_n(\mathbf{x}_1) \\ \phi_1(\mathbf{x}_2) & \phi_2(\mathbf{x}_2) & \cdots & \phi_n(\mathbf{x}_2) \\ \vdots & \vdots & \ddots & \vdots \\ \phi_1(\mathbf{x}_n) & \phi_2(\mathbf{x}_n) & \cdots & \phi_n(\mathbf{x}_n) \end{vmatrix}. \tag{6}$$

For example, in the special case of a two-electron system one obtains

$$\Psi_{SD}(\mathbf{x}_1, \mathbf{x}_2) = \frac{1}{\sqrt{2}}\big(\phi_1(\mathbf{x}_1)\phi_2(\mathbf{x}_2) - \phi_1(\mathbf{x}_2)\phi_2(\mathbf{x}_1)\big)\,, \tag{7}$$

which naturally obeys the Pauli principle:[7]

$$\begin{aligned} \Psi_{SD}(\mathbf{x}_2, r_1) &= \frac{1}{\sqrt{2}}\big(\phi_1(\mathbf{x}_2)\phi_2(\mathbf{x}_1) - \phi_1(\mathbf{x}_1)\phi_2(\mathbf{x}_2)\big) && (8)\\ &= -\frac{1}{\sqrt{2}}\big(\phi_1(\mathbf{x}_1)\phi_2(\mathbf{x}_2) - \phi_1(\mathbf{x}_2)\phi_2(\mathbf{x}_1)\big) && (9)\\ &= -\Psi_{SD}(\mathbf{x}_1, \mathbf{x}_2)\,. && (10) \end{aligned}$$

Plugging the Slater determinant and the Hamilton operator from the previous chapter into the Schrödinger equation, one eventually ends up at the Hartree–Fock equations[8],[9]

$$\hat{F}\phi_i = \epsilon_i \phi_i\,. \tag{11}$$

Where the Fock operator $\hat{F}$ consists of the kinetic energy operator of the electron, the nuclear-electron attraction and the Coulomb and Exchange interaction with the other electrons:

$$\hat{F} = -\frac{1}{2}\Delta + \hat{V}_{Ne} + \hat{J} - \hat{K}\,. \tag{12}$$

This represents a set of coupled equations, one equation per molecular orbital. Here, each electron is treated in the mean field of all other electrons. This necessitates an iterative process to solve the equations: First, an initial set of molecular orbitals is obtained by some sort of educated guess. Then, the Hartree–Fock equations are solved using the mean field of the previously generated molecular orbitals to obtain a new set of MOs. This step is repeated until convergence is reached. The procedure outlined here is called the self-consistent field (SCF) procedure.

The molecular orbitals $\phi_i(\mathbf{x})$ are usually expanded in a linear combination of atomic orbitals (LCAO).[9],[10] Here, a basis set consisting of different atomic orbitals $\chi_\mu(\mathbf{x})$ are chosen for the calculation and the expansion coefficients $c_{i\mu}$ are optimized during the SCF procedure:

$$\phi_i(\mathbf{x}) = \sum_\mu c_{i\mu}\chi_\mu(\mathbf{x})\,, \tag{13}$$

where the sum runs over all atomic orbitals.

2.4 Density functional theory

A major weakness of the Hartree-Fock method is the neglect of electron-correlation effects. Since electrons are only treated in the mean field of all other electrons within the Hartree-Fock theory, the mean distances between then are usually too small and therefore the Coulomb repulsion is too big. In reality one electron would try to prevent being in the vicinity of another electron and vice versa and their movement would therefore be correlated.

One strategy to incorporate electron correlation is the density functional theory (DFT). The underlying idea of the DFT is to describe the energy of the system as a functional of the density $E[\rho]$ instead of a functional of the wave function $E[\Psi]$ like in Hartree–Fock theory. The Hohenberg–Kohn theorem provides the theoretical foundation to know that there exists a functional that gives the exact energy of the system. The exact form of said functional is not know and is therefore approximated in practical calculations. Currently, there is no satisfactory approximation to the kinetic energy functional. To tackle this problem, Kohn and Sham reformulated the DFT and reintroduced orbitals. This makes it possible to calculated the kinetic energy exactly, like in Hartree-Fock theory. In the Kohn–Sham density functional theory[11] (KSDFT) only the exchange and correlation energies are calculated as a functional of the density. There exists a plethora of different approximations to this exchange-correlation (xc) functional with different levels of sophistication.

2.4.1 DFT functional classes

There are a few different classes of DFT functionals, this section gives a quick overview of the respective approaches. For detailed instructions and practical advice regarding functionals, common approximations and additional corrections for DFT calculations using TURBOMOLE, please consult chapter 6 of the manual.[1] The interested reader is referred to textbooks like reference [10]. There are many benchmark studies that compare different functionals in different chemical contexts. For example extensive studies exist for excitation energies using DFT like references [12] or [13].

LDA, GGA and mGGA

The energy functional $E[\rho]$ formally is only dependent on the value of the density ρ itself. Within the Local density approximations (LDA), the approximate functional for practical DFT calculations is also only dependent on the density ρ. Analytical expressions for the correlation and exchange energy of the homogeneous electron gas are known and fall under this category. The offer a very crude approximation for molecular systems as they assume a constant (or at the very least slowly varying) electron density, which is not the case in most molecules.
The general gradient approximation (GGA) makes use of the first derivative of the density $\nabla\rho$ in addition to the density ρ itself. The functional can be written as $E^{\mathrm{GGA}}[\rho, \nabla\rho]$.
In addition to the first derivative of the density, also the second derivative might be considered. Such functionals fall into the meta-GGA (mGGA) class, $E^{\mathrm{mGGA}}[\rho, \nabla\rho, \tau]$. Here, $\tau = \nabla\rho \cdot \nabla\rho$ is

the kinetic energy density. Alternatively, the true Laplacian of the density $\nabla^2\rho = \Delta\rho$ may be used, which is numerically harder to handle that the kinetic energy density, which is why τ is used more widely. Within the growing degree of sophistication of LDAs, GGAs and mGGAs, mGGAs generally offer the best description of the exchange correlation energy of molecular systems.
There is no significant increase in computational cost between LDAs, GGAs and mGGAs. The most time consuming step is still the computation of the electron–electron Coulomb interaction, the exchange interaction is now much cheaper as it is also calculated as a functional of the density. If further approximations are used to the Coulomb interaction, a DFT calculation using the functionals presented in this subsection is much cheaper than a respective Hartree–Fock calculation, while generally providing much better results due to the inclusion of electron correlation effects.

Hybrid functionals

One of the biggest sources of errors remaining for LDA, GGA and mGGA functionals is the self-interaction error of the electrons.[10] In Hartree–Fock theory, Coulomb and exchange interactions of an electron with itself exactly cancel each other, which is the correct physical behavior, as the electron does not interact with itself. The DFT functionals of the previous subsection approximate the exchange interaction as a functional of the density and thus Coulomb and exchange no longer cancel each other completely for one electron. This introduces the so called self-interaction error. To combat this, hybrid functionals include a certain amount of exact Hartree–Fock exchange with the goal of minimizing the self-interaction. Conventional hybrid functionals such as B3LYP or PBE0 always use a fixed amount of Hartree–Fock exchange. There are more advanced types of hybrid functionals such as range-seperated hybrid functionals of local hybrid functionals that use different amounts of Hartree–Fock exchange, based on different heuristics.

2.5 Relativistic effects

For heavy elements like rare-earth elements relativistic effects become important. In comparison with a non-relativistic framework the s- and p-orbitals are more contracted and possess a lower energy. Because of the stronger shielding of the effective core potential the d- and f-levels get destabilized and expanded.[14] There are two types of relativistic effects: scalar relativistic effects and spin–orbit coupling. Scalar relativistic effects only shifts the energy levels while spin-orbit coupling causes a splitting of degenerated energy levels. Scalar relativistic effects can be employed in a one-component framework, for describing spin–orbit coupling we need two-components with complex spinors instead of one-component orbitals.
For relativistic effects we need an equation for quantum mechanic effects which also fullfills the special relativity theory and is invariant under a Lorentz transformation. The Schrödinger equation does not fullfill these requirements. So we need another equation, the Dirac equation. In the following the Dirac equation for a free particle is used. If we want to use the Dirac equation for a molecule a potential has to be added.

$$i\hbar\frac{\partial\Psi_D(r,t)}{\partial t} = [-i\hbar c\vec{\alpha}\vec{\nabla} + \beta mc^2]\Psi_D(r,t) \tag{14}$$

The Ψ_D is the Dirac wave function, m is the mass of the free particle and c is in this case the speed of light. $\vec{\nabla}$ is the Nabla operator. It is a vector operator whose components are the partial derivative operators. The operators α_i and β are 4x4 matrices.

$$\alpha_i = \begin{pmatrix} 0 & 0 & & \\ 0 & 0 & & \sigma_i \\ & & 0 & 0 \\ & \sigma_i & 0 & 0 \end{pmatrix}, \quad \beta = \begin{pmatrix} 1 & 0 & 0 & 0 \\ 0 & 1 & 0 & 0 \\ 0 & 0 & -1 & 0 \\ 0 & 0 & 0 & -1 \end{pmatrix} \tag{15}$$

These matrices include the Pauli matrices σ_i

$$\sigma_x = \begin{pmatrix} 0 & 1 \\ 1 & 0 \end{pmatrix}, \quad \sigma_y = \begin{pmatrix} 0 & -i \\ i & 0 \end{pmatrix}, \quad \sigma_z = \begin{pmatrix} 1 & 0 \\ 0 & -1 \end{pmatrix} \tag{16}$$

Because of the fourdimensional structure of α_i and β the wave function has to have four-components, forming a so called Dirac spinor.

$$\Psi_D(r,t) = \begin{pmatrix} \Psi_1(r,t) \\ \Psi_2(r,t) \\ \Psi_3(r,t) \\ \Psi_4(r,t) \end{pmatrix} \tag{17}$$

For a few calculations we need to use these four-components. These consist of two positron components and two electron components. In chemistry we are only interested in electronic contributions. Therefore, the components can be decoupled with different methods.
For example we can use the X2C approach were only the one-electron part is decoupled. Therefore, we need the one-electron Dirac equation in the finite basis set expansion. This includes electronic and positronic states but we are only interested in the electronic ones. To get a two-component electrons-only equation, we have to diagonalize the one-electron Dirac matrix. For that, we perform a unitary transformation of the Dirac Hamiltonian with the unitary matrix **U**.

$$\mathbf{U} = \begin{pmatrix} 1 & 0 & -\mathbf{X}^\dagger \\ 0 & 1 & \\ \mathbf{X} & & 1 \quad 0 \\ & & 0 \quad 1 \end{pmatrix} \begin{pmatrix} \mathbf{R} & & 0 \quad 0 \\ & & 0 \quad 0 \\ \begin{pmatrix} 0 & 0 \\ 0 & 0 \end{pmatrix} & & \mathbf{R'} \end{pmatrix} \tag{18}$$

Here, **X** is the decoupling matrix and **R** and **R'** are renormalization matrices.[15]
To perform calculations with the X2C approach we have to use the x2c basis sets. These are optimized for this approach. More information about how to perform such calculations with TURBOMOLE and relativistic in general can be found in the manual in chapter 6.4.[1]

2.6 Relativistic effective core potentials (ECP)

As described earlier, relativistic effects like scalar relativistic effects and spin-orbit coupling need to be considered for heavy elements like the lanthanides. Instead of considering all electrons like the all-electron method X2C, one can use so called effective core potentials (in short ECPs) for the electronic description of the lanthanides. An ECP describes the inner electrons with a potential and only the most outer electrons are considered explicitly in the calculation. This basically reduces the Hamilton operator from an all-electron operator to a so called valence-only Hamiltonian

$$\hat{H}_v = \sum_i^{n_v} h_v(i) + \sum_{i<j}^{n_v} g_v(i,j) + V_{cc} + V_{cpp} \tag{19}$$

in which c and v are core and valence contributions, $h_v(i)$ and $g_v(i,j)$ are the respective one- and two-electron operators of the valence electrons while V_{cc} and V_{cpp} describe Coulomb repulsion and the core polarization potential of all cores and their nuclei. This equation already shows that it is possible to exclude certain parts of the working equations with the usage of an ECP which leads to computational savings. Scalar relativistic effects can be included via the one- and two-electron operators

$$h_v(i) = -\frac{1}{2}\Delta_i + V_{cv}(i) \quad \text{and} \quad g_v(i,j) = \frac{1}{r_{ij}}, \tag{20}$$

more specifically by parametrization of the effective core potential V_{cv} of the one-electron operator which describes the interaction of a valence electron with the nuclei of the regarded system. There are two different types of ECPs which are called small-core or large-core ECPs. They only differ in the amount of electrons covered by the potential.
In Section 3 of this article, scalar relativistic large-core ECPs of Wood-Boring type developed by *Dolg* et al.[16] were used which include not only the most inner electrons but also the f electrons in the ECP. This is a very, if not the most important, aspect for lanthanides due to their high number of unpaired electrons which leads to strong convergence problems. Because each lanthanide usually has a different number of f electrons, one has to use a different ECP for each different f occupation,

labeled as f^n, f^{n-1} or f^{n-2} in the following. As a project of this CRC, we optimized error-consistent basis sets[17] for the usage in conjunction with large-core ECPs from *Dolg* et al. similar to the def2 series.[18] For a more detailled insight into effective core potentials we refer to the work of *Dolg*, especially his overview article of ECPs.[19]

3 DFT calculations on Lanthanides in practice

3.1 Atoms

The ground state of the majority of Ln atoms is $f^n s^2$, e.g. $f^{14}s^2$ for Yb or $f^7 s^2$ for Eu. Exceptions are Ce, Gd and Lu, which exhibit ($f^{n-1}s^2d^1$) ground states ($f^1s^2d^1$, $f^7s^2d^1$, $f^{14}s^2d^1$), as well as La itself ($f^0s^2d^1$). These preferences are reproduced only by a few quantum chemical methods, as demonstrated in the following atomic calculations. For adjusting the occupation of the f shell, we choose C_i symmetry. Here, the f (and p) orbitals transform as a_u and the s (and d) orbitals) transform as a_g. In Table 1 the occupations for $f^n s^2$ and $f^{n-1}s^2d^1$ are shown, and the energy difference between the two states, $\Delta = E(f^{n-1}s^2d^1) - E(f^n s^2)$, as obtained with scalar X2C[20] employing the finite nucleus model and x2c-TZVPall basis sets[21] with the pure DFT functionals PBE as well as with the hybrid functional PBE0 (for practical hints see end of this section).

Table 1: Occupation in C_i symmetry and energy difference Δ between the states $f^n s^2$ and ($f^{n-1}s^2d^1$) in eV for PBE0 and PBE for all lanthanides ($\Delta > 0$ means a preference of the $f^n s^2$ state). In the columns AP it is noted whether the Aufbau principle is fulfilled (o) or not (x). The first letter refers to the $f^n s^2$ state, the second to the ($f^{n-1}s^2d^1$) state.

	$f^n s^2$					$f^{n-1}s^2d^1$					PBE0		PBE	
	α		β		n_α-n_β	α		β		n_α-n_β				
	a_g	a_u	a_g	a_u		a_g	a_u	a_g	a_u		Δ / eV	AP	Δ / eV	AP
Ce	16	**14**	16	12	2	17	**13**	16	12	2	0.00	oo	0.29	xx
Pr	16	**15**	16	12	3	17	**14**	16	12	3	0.83	oo	1.71	xx
Nd	16	**16**	16	12	4	17	**15**	16	12	4	1.46	oo	1.95	ox
Pm	16	**17**	16	12	5	17	**16**	16	12	5	1.81	oo	2.40	ox
Sm	16	**18**	16	12	6	17	**17**	16	12	6	2.83	ox	3.34	ox
Eu	16	**19**	16	**12**	7	17	**18**	16	12	7	3.72	ox	4.15	ox
Gd	16	19	16	**13**	6	17	**19**	16	**12**	8	-0.84	oo	0.33	xx
Tb	16	19	16	**14**	5	17	19	16	**13**	7	0.17	oo	1.17	xx
Dy	16	19	16	**15**	4	17	19	16	**14**	6	1.15	oo	2.01	ox
Ho	16	19	16	**16**	3	17	19	16	**15**	5	1.40	oo	2.37	ox
Er	16	19	16	**17**	2	17	19	16	**16**	4	1.36	oo	2.45	ox
Tm	16	19	16	**18**	1	17	19	16	**17**	3	2.29	oo	3.23	ox
Yb	16	19	16	**19**	0	17	19	16	**18**	2	3.18	ox	4.01	ox
Lu	-	-	-	-		17	19	16	**19**	1	-	-o	-	-o

The preference of the ($f^{n-1}s^2d^1$) ground state for Gd is correctly predicted only by the hybrid functional, meanwhile for Ce, which is the other lanthanide with an ($f^{n-1}s^2d^1$) ground state, the hybrid functional at least predicts equal energies for both states, whereas according to the pure DFT functional the $f^n s^2$ state is favourable. Even more problematic for pure functionals is the violation of the Aufbau principle (i.e. negative HOMO–LUMO gaps): For Ce, Pr, Gd and Tb this happens for both states, reflecting that the usage of pure DFT functionals at least for some of the lanthanides obviously is problematic already for the atoms. PBE0 in contrast does a very reasonable job; the violation of the Aufbau principle for the ($f^{n-1}s^2d^1$) state in case of Sm, Eu and Yb is expected, as for these elements this state is highly de-preferred over the $f^n s^2$ state.

3.2 Ln(III) compounds

In most Ln compounds the lanthanide adopts the (formal) oxidation state +III. As an example, we calculated all LnH_3 compounds in planar structure assuming D_{3h} symmetry. For this point group, the seven f orbitals transform as $a_1' \bigoplus a_2' \bigoplus a_2'' \bigoplus e' \bigoplus e''$ and the three Ln-H bonds as $a_1' \bigoplus e'$ (thus, a mixture of f orbitals and bonds cannot be forbidden by symmetry). We have chosen the f occupation that yields the lowest energy (second column in Table 2) and optimized the Ln-H distance. For the optimized structure we list the average orbital energy of the $a_1' \bigoplus e'$ orbitals representing mainly the bonds, ϵ(bonds), and that of the orbitals mainly containing the Ln(f) electrons, ϵ(f), further the total f occupation, n(f) and the f contribution to the bond orbitals, n_b(f), obtained by a Mulliken analysis. This was done for PBE0 and PBE. For PBE0, the Ln(f) orbitals are energetically well separated from the bond orbitals (Ce is an exception) and the calculated f occupation is always close to n-1 (also for Ce), i.e. there are only very small contributions of Ln(f) to the bond. The Aufbau principle is fulfilled throughout. Everything meets the expectations. This is by far not the case for PBE. For Ce to Pm the f orbitals are even higher in energy than the bond orbitals and also for the subsequent elements the energetic separation is not large (except for Lu). Consequently, one observes a relatively large mixing of Ln(f) orbitals and bond orbitals, and often the Aufbau principle is not fulfilled. It is obvious that pure DFT functionals are not well suited for all-electron treatments of lanthanides (with the exception of Lu).

Table 2: The occupation of LnH_3 molecules in D_{3h} symmetry is given in the second to sixth column, "1" means half-occupied, "2" means fully occupied. ϵ(bonds) is the average orbital energy in eV of the $a_1' \bigoplus e'$ orbitals representing the bonds, and ϵ(f) that of the orbitals containing the Ln(f) electrons. N(f) is the total f occupation, n(f) and the f contribution to the bond orbitals, n_b(f), obtained by a Mulliken analysis. In the column AP it is noted whether the Aufbau principle is fulfilled (o) or not (x). Both data for PBE and PBE0 refer to structure parameters obtained with PBE (X2C, x2c-TZVPall bases).

	occupation					PBE0					PBE				
	a_1'	a_2'	a_2''	e'	e''	ϵ(f)	ϵ(bonds)	n(f)	n_b(f)	AP	ϵ(f)	ϵ(bonds)	n(f)	n_b(f)	AP
Ce	0	0	1	0	0	-6.71	-6.97	1.16	0.16	o	-3.74	-5.77	1.19	0.24	x
Pr	0	1	1	0	0	-8.19	-6.99	2.17	0.18	o	-4.71	-5.78	2.27	0.38	o
Nd	0	0	1	0	1	-8.99	-7.08	3.20	0.20	o	-5.09	-5.85	3.34	0.37	o
Pm	0	1	1	0	1	-9.98	-7.10	4.22	0.22	o	-5.42	-5.87	4.43	0.47	o
Sm	0	1	0	1	1	-11.09	-7.16	5.16	0.18	o	-6.67	-5.90	5.34	0.46	x
Eu	0	1	1	1	1	-10.89	-7.20	6.29	0.30	o	-6.34	-5.93	6.47	0.76	x
Gd	1	1	1	1	1	-13.41	-7.30	7.05	0.07	o	-9.31	-6.07	7.14	0.20	o
Tb	1	1	2	1	1	-13.07	-7.38	8.05	0.06	o	-8.80	-6.14	8.17	0.21	x
Dy	1	2	2	1	1	-13.00	-7.40	9.05	0.07	o	-8.10	-6.14	9.25	0.32	o
Ho	1	1	2	1	2	-12.77	-7.49	10.07	0.08	o	-7.70	-6.20	10.28	0.33	x
Er	1	2	2	1	2	-12.83	-7.51	11.08	0.09	o	-7.08	-6.22	11.37	0.49	o
Tm	1	2	1	2	2	-13.14	-7.58	12.04	0.05	o	-8.16	-6.27	12.22	0.32	x
Yb	1	2	2	2	2	-12.92	-7.64	13.06	0.08	o	-7.04	-6.27	13.36	0.76	x
Lu	2	2	2	2	2	-13.45	-7.70	14.00	0.03	o	-9.96	-6.48	13.99	0.05	o

As long as one is sure about the f occupation, effective core potentials that cover the electrons in the f shell are a highly attractive alternative to all-electron relativistic treatments, at least as long as one is not specifically interested in the f electrons. In the course of the CRC we integrated these so-called large-core ECPs[16],[22] in the library of our program suite Turbomole, named those for the f^{n-1} occupation "lcecp-1", and designed and optimized basis sets in the sense of our system of error-balanced basis sets, named lcecp-1-SVP, lcecp-1-TZVP and lcecp-1-QZVP.[17]

Table 3: Ln-H distances of LnH_3 compounds (in pm) calculated in D_{3h} symmetry with the all-electron scalar relativistic X2C method with corresponding basis sets x2c-TZVPall at PBE0 level and with large-core ECPs for f^{n-1} occupations, lcecp-1, and corresponding newly designed and optimized basis sets lcecp-1-TZVP at levels PBE0 and PBE.

	X2C/TZVP/PBE0	Lcecp-1/TZVP/PBE0	Lcecp-1/TZVP/PBE
Ce	207.44	209.19	209.61
Pr	205.57	207.64	208.08
Nd	204.22	206.18	206.62
Pm	203.23	205.27	205.67
Sm	202.83	204.23	204.63
Eu	203.76	203.12	203.50
Gd	200.97	202.16	202.54
Tb	199.58	201.09	201.47
Dy	198.57	200.18	200.55
Ho	197.31	199.21	199.60
Er	196.56	198.26	198.66
Tm	195.98	197.43	197.84
Yb	194.97	196.49	196.91
Lu	194.33	196.35	196.77

They are not yet published and thus available only upon request, nevertheless we compare the structure parameters of LnH_3 with all-electron relativistic treatments (see above) and ECP treatments in Table 3. We observe a consistent difference of $\sim$2 pm, except for Eu, for which X2C and lcecp are almost identical. Further, we see excellent agreement between PBE0 and PBE, as the problematic f electrons no longer are explicitly treated.

3.3 Overall summary and practical hints

As long as one is sure about the f occupation (in particular f^{n-1}) and is not specifically interested in the f electrons, thus e.g. when structure-optimizing Ln(III) compounds, LCECPs are the means of choice. Here the highly efficient pure DFT functionals are as good as hybrid functionals. However, if one is either interested in the f electrons or even in the inner shells or is not sure about the f occupation, or is interested in reaction or atomization energies (where the f occupation usually changes), all-electron relativistic treatments are necessary. Recommended basis sets are x2c-TZVPall, keywords to be added to the control file are \$rx2c, \$finnuc and \$rlocal. The usage of pure DFT functionals is not recommended for this approach. For the determination of the occupation one may try Fermi smearing, preferably with a fixed number of electrons, e.g. for a compound with two Pr atoms in presumed f^{n-1} states. For this, one needs to add the keyword \$fermi with default values and nue=4 for the number of unpaired electros (but you can also try other values, sometimes this yields better results).

4 Calculation of HFC constants on Lanthanide complexes

Open-shell Ln compounds exhibit magnetic properties, which can be investigated by electron paramagnetic resonance (EPR) spectroscopy. EPR spectra are generally interpreted with the help of spectroscopic parameters, like the hyperfine-coupling (HFC) tensor $\boldsymbol{A}$ and the g-tensor.[23] These tensors can be calculated using quantum-chemical methods, which is subject of research for quite a while now (see e.g. Ref. [24] as an early overview). Within the framework of DFT, a prerequisite for these kinds of calculations are converged molecular orbitals. The focus on this section lies on the HFC tensor and its isotropic HFC constant, as the calculation of this property, especially of the HFC constant, works quite reliably in certain cases. Details on the calculation of EPR properties with Turbomole can be found in chapter 18 of the Turbomole manual for version 7.8.[1]

The HFC tensor for the nucleus N $\boldsymbol{A}_N$ describes the interaction between the nuclear spin of nucleus N $\vec{I}_N$ and the electronic spin $\vec{S}$ in the HFC Hamiltonian

$$\hat{H}_N^{\mathrm{HFC}} = \vec{I}_N \, \boldsymbol{A}_N \, \vec{S} \, . \tag{21}$$

The isotropic HFC constant is then calculated out of the tensor via

$$A_N^{\mathrm{iso}} = \frac{1}{3}\mathrm{Tr}(\boldsymbol{A}_N) = \frac{1}{3}(A_{N,xx} + A_{N,yy} + A_{N,zz}) \, . \tag{22}$$

Within the framework of DFT, there are several ways of calculating the HFC tensor, depending on the way scalar relativistic effects and spin–orbit coupling are treated. ECPs should not be chosen for the calculation, as the electrons close to the nucleus play an important role for the HFC. For lanthanides, a complete neglect of relativistic effects is not advisable either. Within TURBOMOLE, an implementation for a two-component (2c) calculation of the HFC tensor in the framework of exact two-component (X2C) theory is available.[25] However, using a one-component (1c) approach within X2C (with[26] or without[27] consideration of a spin–orbit perturbation) for the calculation of the HFC is more easy to apply for general users, computationally more efficient, and often sufficient.

There are several contributions to the HFC tensor, which are often discussed separately. However, they can only really be separated within a non-relativistic framework, which is why in the following non-relativistic expressions are given (see e.g. Ref. [28]). For the relativistic expressions within X2C, see refs. [25]–[27]. The equations are given in atomic units and assume point nuclear charges.

The first contribution to the HFC tensor is the isotropic Fermi contact contribution, given by

$$A_N^{\mathrm{FC,iso}} = \frac{4\pi}{3c^2} \frac{g_e \mu_{\mathrm{B}} g_N \mu_{\mathrm{N}}}{S} \sum_{\mu,\nu} \mathrm{P}_{\mu\nu}^{\alpha-\beta} \, \langle \phi_\mu | \, \delta(\vec{r}_N) \, | \phi_\nu \rangle \, . \tag{23}$$

Here, c is the speed of light, g_e is the g-factor of the free electron, μ_{B} is the Bohr magneton, g_N is the g-factor of the respective nuclear spin, μ_{N} is the nuclear magneton, ϕ_μ are basis functions, $\mathrm{P}_{\mu\nu}^{\alpha-\beta}$ is the excess spin-density matrix, $\delta(\vec{r}_N)$ is the Dirac delta function, and $\vec{r}_N$ is the position vector of the electron relative to the nucleus N. The summation on the right side of the equation gives the excess spin-density $\rho^{\alpha-\beta}$ at the nuclear position. In other words, the FC contribution depends on the excess spin-density at the nucleus and becomes zero, if no excess spin-density is found at the nucleus.

The second contribution is the spin–dipolar (SD) term, which describes the dipole–dipole interaction between the electronic and the nuclear spin. It is given by

$$A_{N,uv}^{\mathrm{SD}} = \frac{1}{2c^2} \frac{g_e \mu_{\mathrm{B}} g_N \mu_{\mathrm{N}}}{S} \sum_{\mu,\nu} \mathrm{P}_{\mu\nu}^{\alpha-\beta} \, \langle \phi_\mu | \frac{3 r_{N,u} r_{N,v} - r_N^2 \delta_{uv}}{r_N^5} | \phi_\nu \rangle \, , \tag{24}$$

where u, v are Cartesian components and r_N is the distance between the electron and nucleus N. The SD contribution is completely anisotropic and does not contribute to A_N^{iso}. This is why A_N^{iso} and $A_N^{\mathrm{FC,iso}}$ are assumed to be the same in cases where spin–orbit coupling is not considered. In scalar relativistic X2C calculations, i.e. under neglect of spin–orbit coupling, the FC and SD contributions appear in a coupled form and are obtained separately within the non-relativistic limit.

Spin–orbit coupling can be treated self-consistently within a 2c framework or perturbatively in a scalar relativistic or non-relativistic framework. The non-relativisitc paramagnetic spin–orbit (PSO) term, which is the result of the perturbative treatment, is given by

$$A_{N,uv}^{\mathrm{PSO}} = \frac{1}{c^2} \frac{g_e \mu_{\mathrm{B}} g_N \mu_{\mathrm{N}}}{S} \sum_{\mu,\nu} \mathrm{P}_{\mu\nu}^{\alpha-\beta(v)} \, \langle \phi_\mu | \frac{(\vec{r}_N \times \hat{\vec{p}})_u}{r_N^3} | \phi_\nu \rangle \, , \tag{25}$$

where $\mathrm{P}_{\mu\nu}^{\alpha-\beta(v)}$ is the perturbed excess spin-density matrix with respect to a spin–orbit perturbation in the Cartesian v direction and $\hat{\vec{p}}$ is the momentum operator. The PSO term might give isotropic and anisotropic contributions to the whole HFC tensor. Therefore, A_N^{iso} and $A_N^{\mathrm{FC,iso}}$ cannot be assumed to be completely the same if spin–orbit coupling is considered.

When considering the results of an HFC tensor calculation, often only the isotropic HFC constant A_N^{iso} or the three principal components, $A_{N,11}$, $A_{N,22}$, and $A_{N,33}$ are discussed. The principal components are obtained either by aligning the molecule with its principal axes of inertia, so that the calculated HFC tensor is diagonal, or by diagonalizing the resulting HFC tensor. Within TURBOMOLE, the diagonalization of the tensor is just done with the symmetric part of the total HFC tensor, as the antisymmetric part is usually negligible for the diagonalization. In order to avoid this small error, the molecule can be aligned with its principal axes of inertia within the `define` environment of TURBOMOLE. Note that a good agreement with experiment for A_N^{iso} may not necessarily lead to the same quality of agreement for the principal components, as error cancellation may occur.

The calculation of HFC constants on lanthanide compounds with the spin–orbit perturbation approach is reliable—for up to now considered cases—if a) the unpaired electrons are mainly located on the lanthanide and b) the unpaired electrons are mostly of s- and d- (and not f-) character. This results in an applicability mostly for single-center La(II) and Lu(II) complexes with one unpaired electron. For other cases, a simple 1c black-box DFT approach might not be sufficient for the calculation.

As an example, calculated and experimental results for the HFC constants of three lanthanide single-molecule magnets, which are novel candidates for molecular qubits and are depicted in Figure 1, are shown in Figure 2. These complexes were studied experimentally in Ref. [29]. The calculations are taken from Ref. [26]. It can be seen that good agreement with the experimental values is obtained and that even a scalar relativistic approach would be sufficient in this case.

Note that calculations for the EPR g-tensor are also available within TURBOMOLE, both with a perturbative and a 2c approach (see chapter 18 of the TURBOMOLE manual[1] for details). However, the errors are generally a bit larger and a 2c approach is generally recommendable, as the impact of spin–orbit coupling on the g-tensor is larger than on the HFC tensor.

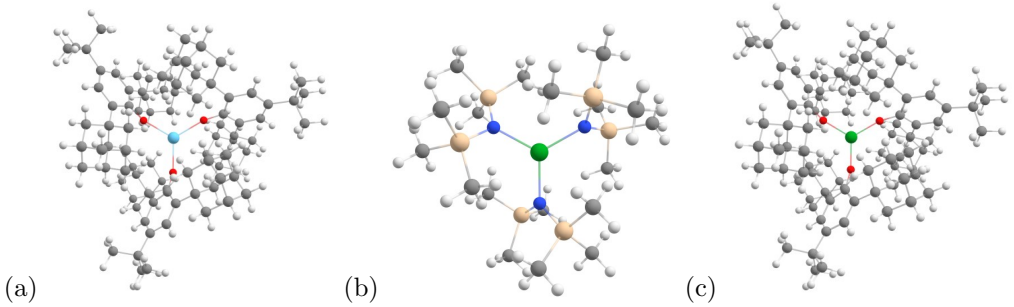

Figure 1: Depiction of (a) $[\mathrm{La(OAr^*)_3}]^-$, (b) $[\mathrm{Lu(NR_2)_3}]^-$, (c) $[\mathrm{Lu(OAr^*)_3}]^-$ ($\mathrm{OAr^*}$ = 2,6-$\mathrm{Ad_2}$-4-^{t}Bu-$\mathrm{C_6H_2O}$, with Ad = adamantyl and ^{t}Bu = *tert*-butyl, R = $\mathrm{SiMe_3}$). White: H, grey: C, blue: N, red: O, brown: Si, light blue: La, green: Lu.

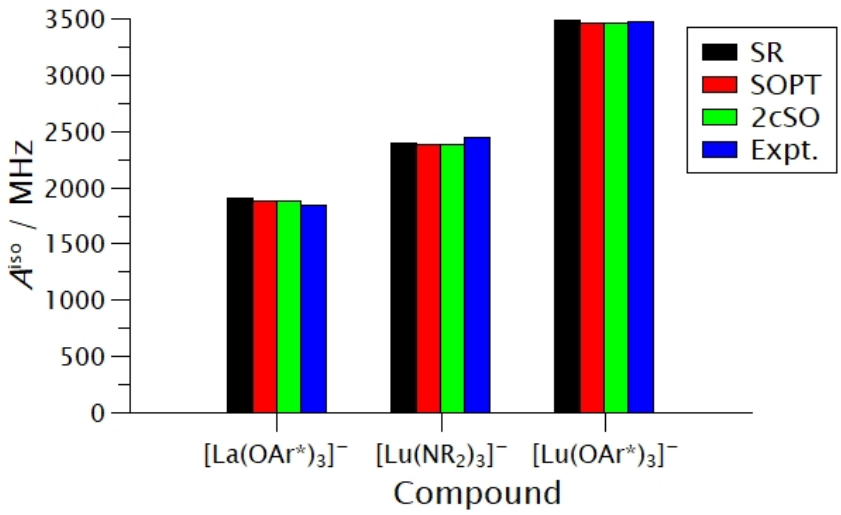

Figure 2: Comparison between calculated and experimental isotropic HFC constants for $[La(OAr^*)_3]^-$, $[Lu(NR_2)_3]^-$, and $[Lu(OAr^*)_3]^-$. SR: scalar relativistic X2C approach, SOPT: perturbative treatment of spin–orbit coupling within X2C, 2cSO: 2c X2C approach, Expt.: experimental values. Note that the experimental uncertainty amounts to 25 MHz for $[La(OAr^*)_3]^-$ and to 50 MHz for the other two complexes. For the calculations, the x2c-TZVPall-2c basis set[21] was used for the central Ln atom, while x2c-SVPall-2c[21] was used for the light atoms. The ωB97X-D functional[30] was employed.

5 Accurate calculations of atomic spectroscopic properties using GRASP2018

As previously discussed, non-negligible relativistic contributions arise within the regime of lanthanoids. The investigation of spectroscopic properties of lanthanoid ions consequently require explicit relativistic treatment as well as an approach accounting for the large contribution of the electron correlation. The program package `GRASP2018` provides the necessary framework with a four-component approach in theory and additional *quantum electrodynamics* (QED) corrections, allowing accurate predictions of energy levels and transition strengths. Additionally, crystal field calculations are available as well.
The correct usage of `GRASP2018` is non-trivial due to its vast options regarding the choice of the active space. This article aims to provide guidelines for an informed usage with the ultimate goal to obtain accurate and physical meaningful results. One should refer to the manual if a more in-depth description for the user prompts is desired. The manual can be found on the GitHub site of the CompAs group: `https://github.com/compas/grasp/releases/tag/2018-12-03`.
Further information regarding mathematical expressions are provided in Ref. [31] and Ref. [32] for additional insights to the computational strategies as presented in this article.

5.1 Brief theoretical background

The required level of theory has to account for spin–orbit coupling that results as the magnetic momentum of an electron interacting with the effective magnetic field that results from the electronic motion around the atomic core.[33] The magnitude of the spin–orbit coupling scales with Z^4[33] and surpasses the coulombic interaction for heavy atoms. Commonly, three regimes are used to describe the magnitude of the spin–orbit coupling:[34]

1. weak: $\hat{H}^{\mathrm{C}} >> \hat{H}^{\mathrm{SO}}$
   The spin–orbit coupling is orders of magnitude weaker than the coulombic force. L and S are good quantum numbers and the Russell–Saunders/LSJ coupling can be applied.
2. intermediate: $\hat{H}^{\mathrm{SO}} \approx \hat{H}^{\mathrm{C}}$
   The spin–orbit coupling and coulombic force are of similar order of magnitude. Commonly, Russel–Saunders coupling is employed. However, the ${}^{2S+1}L$ terms are no longer degenerate and form ${}^{2S+1}L_J$ multipletts. Additionally, the seniority quantum number ν is introduced to differentiate between terms with the same S and L quantum number ${}^{2S+1}L_J\nu$.
3. strong: $\hat{H}^{\mathrm{C}} << \hat{H}^{\mathrm{SO}}$
   The spin–orbit coupling is orders of magnitude stronger than the coulombic force as it is the case for e.g. heavy elements. L and S are no longer good quantum numbers, therefore the jj coupling has to be applied.

Lanthanoids fall into the regime of intermediate coupling.[34] As a consequence, one needs to describe the terms and energy level with the seniority quantum number ν,[31] as e.g. for the first excited state of Eu^{3+} that is ${}^5D3_J$.[35] Additionally, fine-structure splitting arises leading to non-degenerate shells of different quantum number j, e.g. $2p_{1/2}$ being energetically lower than $2p_{3/2}$ as shown in Figure 3.[36] Therefore, calculations with `GRASP2018` are carried out by applying the jj coupling scheme. The energy levels are transformed to the easier comprehensible LSJ coupling only at the end of the calculations.

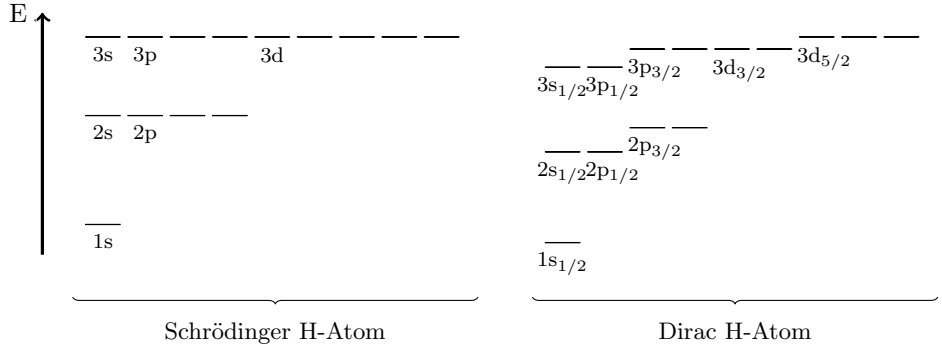

Figure 3: Qualitative spectrum of the hydrogen atom from the Schrödinger and Dirac approach.[36]

`GRASP2018` additionally provides QED corrections. These corrections do not require additional computation time and resources and are advised to be always applied, even though the corrections are usually in the order of up to 2 cm^{-1}. Available QED corrections include transverse photon interaction, vacuum polarization, self-energy, normal and specific mass shift.[31] Therefore, all significant corrections of lower order are included, resulting in an employed Dirac–Coulomb–Breit Hamiltonian[31] with QED corrections that provides are highly accurate level of theory:

$$\hat{H}^{\mathrm{DCB+QED}} = \underbrace{\hat{H}^{\mathrm{DC}} + \hat{H}^{\mathrm{TP}}}_{\hat{H}^{\mathrm{TP}} \simeq \hat{H}^{\mathrm{B}} = \hat{H}^{\mathrm{DCB}}} + \hat{H}^{\mathrm{VP}} + \hat{H}^{\mathrm{SE}} \tag{26}$$

`GRASP2018` uses spectroscopic notation to label the one-electron functions as shown in Table 4.[31] The electronic wave function Ψ is approximated by `GRASP2018` as *Atomic State Function* (ASF) by linear combination of *Configuration State Functions* (CSF) Φ and expansion coefficients $c_i^{\Gamma J}$:[31]

$$\Psi = \sum_i^{N_{\mathrm{CSF}}} c_i^{\Gamma J} \cdot \Phi_i \tag{27}$$

	s	p-	p	d-	d	f-	f	...
	$s_{1/2}$	$p_{1/2}$	$p_{3/2}$	$d_{3/2}$	$d_{5/2}$	$f_{5/2}$	$f_{7/2}$	...
l	0	1	1	2	2	3	3	...
j	$1/2$	$1/2$	$3/2$	$3/2$	$5/2$	$5/2$	$7/2$	...
κ	-1	1	-2	2	-3	3	-4	...

Table 4: Spectroscopic notation (upper line) of the relativistic orbitals (lower line) and their corresponding quantum numbers l, j, κ.

The CSFs are constructed by another linear combination of Slater determinants Ψ_k^{SD} and result by angular momentum coupling of orbitals in a certain configuration. Consequently, the number of CSFs is dependent on the configuration.[31]

$$\Phi_i = \sum_k B_{ki} \cdot \left|\Psi_k^{\mathrm{SD}}\right\rangle \tag{28}$$

5.2 How to use GRASP2018

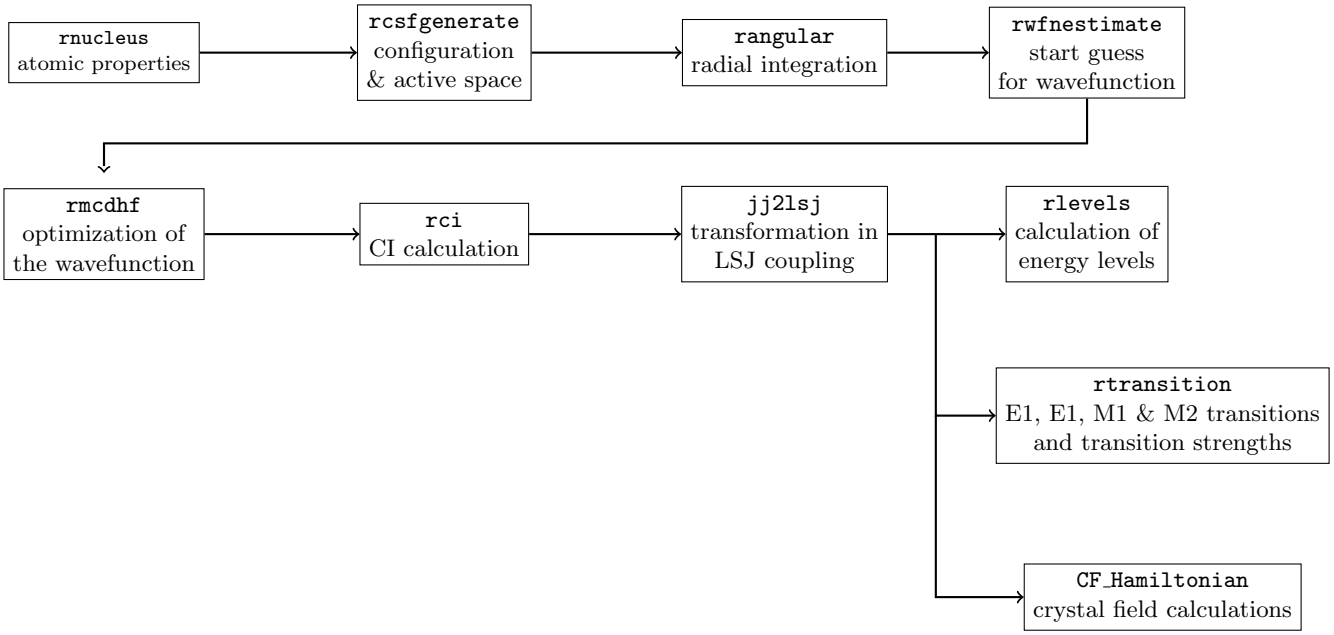

Figure 4: Workflow to calculate energy levels using, transition strengths and perform crystal field calculations with GRASP2018.[37]

A typical workflow with GRASP2018 is depicted in Figure 4 as the program package uses separate modules for each task.[38]
The calculation starts by providing the atomic properties, configuration and active space. The choice on the appropriate configurations and active space (orbital space, order of excitation) heavily influence the required computation time and accuracy:

1. **Configuration**

   (a) multi reference vs. single reference
   One has the option to provide only one configuration (single reference) or several configurations of the same parity (multi reference). Configurations of even and odd parities do

not influence each other[38] and only account to energy levels of the same parity.
e.g. The configuration $4f^6$ of Sm^{2+} is an even configuration and results in the even energy levels ^7F and $^5D3$. $4f^55d^1$ is an odd configuration with several odd energy levels like $^7H^\circ$.[35]

It is highly depending on the system if a multireference approach is required. Hence, it is advised to perform explorativ, cheaper calculations with single reference and different multi reference approaches at the beginning. The results of these calculations should be compared with each other and, if available, with experimental data before approaching accurate and more expensive calculations.
e.g. The even ground state ^7F and first excited state $^5D3$ of Sm^{2+} are best calculated with a single reference approach by using the configuration $4f^6$. Additional even configurations like $4f^45d^2$ occur around 100 000 cm^{-1} and upwards, therefore do not influence the lower lying states.

(b) Correlation
When providing a configuration, the user has to decide whether an orbital is active, inactive or a core orbital. In most cases, inactive and core orbitals have the same effect by them being not used to generate CSFs.
Correlation arises once the number of electrons in active orbitals is two or higher. Three different types of correlation results, depending if the interacting electrons populate a core or valence orbital:[32] valence–valence, core–valence and core–core correlation. It is important for a balanced calculation to account for all three types of correlation by using active core and valence orbitals.

2. **Orbital space**
The orbital space consists of the core, valence and empty virtual orbitals. Adding virtual orbitals increases the number of possible excitations. It is advised to at least add one layer of virtual orbitals, e.g. 6s, 6p, 5d, 5f,5g for Sm^{2+}.

3. **Order of excitation**
Excitations are referred as Singles (S) for exciting one electron to an energetically higher orbital, Doubles (D) for exciting two electrons, Triples (T) for exciting three electrons and so forth. By setting the number of excitations to 2 one allows Singles and Doubles excitation (SD). It is advised to not solely use Singles excitation since these do not provide improvements with larger active spaces (see for further reasoning Brillouin's theorem[39]). Hence, at least SD excitations are advised.

More active orbitals, an larger orbital space and higher orders of excitation result in a larger amount of CSFs and therefore increase the cost of the calculation. It might be helpful to explore the limits of every parameter and determine the most influential parts of the active space. This can be done by observing the convergence behavior of the parameter.
e.g. Increasing the order of excitation for Sm^{2+} reaches convergence once quadruple excitations are applied. However, triples as well as quadruples excitation result in significantly smaller changes than doubles excitation and therefore singles doubles (SD) excitation is sufficiently.

After providing the desired configurations and active space, the calculation continues with the radial integration. The resulting data is written onto the disk. Larger numbers of CSFs may result in a significant amount of required disk space and higher computation time.

Afterwards, a start guess for the wavefunction is needed. Such a start guess can be set up by using the `hf` module to obtain Hartree–Fock orbitals (only works for s, p and d orbitals), recycling an already existing wavefunction `rwfn.out` from another calculation as well as by choosing the options `2`, `3` or `4` within the modules options.

The concluding optimization with `rmcdhf` should usually be performed with the given default settings. If a larger orbital space is desired, then the virtual orbitals should be gradually added as layers, each layer should be optimized before adding another layer and the lower layers should not be reoptimizied when perfoming the optimization for higher layers. Elsewise, problems with convergence will arise.
e.g. An orbital space of 7s, 7p, 6d, 6f, 6g is wanted for Sm^{2+}: first 5s, 5p, 4d, 4f are added and all orbitals are optimized; the resulting wavefunction is reused as a start guess, the orbitals 6s, 6p are added and only 6s, 6p are optimized; the wavefunction is reused again to gradually add 5d, 5f, 7s, 7p, 6d, 6f and 6g. Orbitals with higher angular momentum, like 5d and 5f, might be added indiviually due to convergence problems.

It is advised to use all given QED corrections for the CI calculation with `rci`. Using `jj2lsj` and `rlevels` will provide the results in the comprehensible LSJ coupling.
Afterwards, allowed E1, E2, M1 and M2 transitions and their transition strengths can be calculated using the module `rtransition`.

Crystal Field Calculations
Although no information are provided within the manual, an additional module for crystal field calculations is available under: `https://github.com/compas/cf_hamiltonian`. A detailed explanation can be found in Ref. [40] which is also available under `https://github.com/compas/cf_hamiltonian/tree/main/docs`.
Prepare the input file `Crystaldata` which contains the x, y, z position and the charge of the atoms. The file has to be created by the user themselves.

`Tm(1) Br(3) SYMMETRY = NO 4 1.00 CART`	The first line of the file contains: name of the crystal symmetry, always set to `NO` total number of atoms scaling factor for the coordinates (here `1.00` character type of the coordinates (here cartesian)

`0.000000E+00 0.000000E+00 1.000000E+00 3.000000E+00`
 	
`2.581000E+00 0.000000E+00 1.000000E+00 -1.000000E+00`
⋮
	Second line contains:
	x, y, z positions and charge of the first atom (here Tm^{3+})
	x, y, z positions and charge of the second atom (here Br^{-})

Table 5: Structure of the `Crystaldata` file required to run `CF_Hamiltonian`.

Use the command `CF_Halimtonian` to start the module. The resulting Stark level splitting is listed in the .cCF-Hamil file.

References

[1] TURBOMOLE User's Manual Version 7.8.
Available: `https://www.turbomole.org/turbomole/turbomole-documentation/` [June 24th, 2024], 2023.

[2] E. Schrödinger, *Ann. Phys.*, vol. 384, pp. 361–376, 1926.

[3] E. Schrödinger, *Ann. Phys.*, vol. 385, pp. 437–490, 1926.

[4] M. Born and R. Oppenheimer, *Ann. Phys.*, vol. 389, pp. 457–484, 1927.

[5] R. Van Dyck, F. Moore, D. Farnham, and P. Schwinberg, *International Journal of Mass Spectrometry and Ion Processes*, vol. 66, pp. 327–337, 1985.

[6] J. C. Slater, *Phys. Rev.*, vol. 34, pp. 1293–1322, 1929.

[7] W. Pauli, *Z. Phys.*, vol. 31, pp. 765–783, 1925.

[8] V. Fock, *Z. Phys.*, vol. 61, pp. 126–148, 1930.

[9] A. Szabo and N. S. Ostlund, *Modern Quantum Chemistry: Introduction to Advanced Electronic Structure Theory*. Mineola, NY, US: Dover Publications, 1996.

[10] F. Jensen, *Introduction to Computational Chemistry*, Third edition. Chichester, UK; Hoboken, NJ, US: John Wiley & Sons, 2017.

[11] W. Kohn and L. J. Sham, *Phys. Rev.*, vol. 140, A1133–A1138, 1965.

[12] A. D. Laurent and D. Jacquemin, *International Journal of Quantum Chemistry*, vol. 113, no. 17, pp. 2019–2039, 2013.

[13] D. Jacquemin, V. Wathelet, E. A. Perpète, and C. Adamo, *Journal of Chemical Theory and Computation*, vol. 5, no. 9, pp. 2420–2435, 2009.

[14] M. K. Armbruster, *Entwicklung und Implementierung zweikomponentiger Hartree-Fock- und Dichtefunktionalmethoden*. Ph.D. thesis, Karlsruhe, Forschungszentrum Karlsruhe, 2007.

[15] Y. J. Franzke, N. Middendorf, and F. Weigend, *The Journal of Chemical Physics*, vol. 148, 2018.

[16] M. Dolg, H. Soll, A. Savin, and H. Preuss, *Theor. Chim. Acta*, vol. 75, pp. 173–194, 1989.

[17] F. Weigend and M. Lukanowski, manuscript in preparation, 2024.

[18] F. Weigend and R. Ahlrichs, *Phys. Chem. Chem. Phys.*, vol. 7, pp. 3297–3305, 2005.

[19] M. Dolg, *Modern Methods and Algorithms of Quantum Chemistry: Effective Core Potentials*. NIC Series (NIC-Directors), 2000, vol. 3, pp. 507–540.

[20] D. Peng, N. Middendorf, F. Weigend, and M. Reiher, *The Journal of chemical physics*, vol. 138, 2013.

[21] P. Pollak and F. Weigend, *J. Chem. Theory Comput.*, vol. 13, pp. 3696–3705, 2017.

[22] M. Dolg, H. Stoll, and H. Preuss, *Theor. Chim. Acta*, vol. 85, pp. 441–450, 1993.

[23] M. M. Roessler and E. Salvadori, *Chem. Soc. Rev.*, vol. 47, pp. 2534–2553, 2018.

[24] M. Kaupp, M. Bühl, and V. G. Malkin, Eds., *Calculation of NMR and EPR Parameters. Theory and Applications*. Weinheim, DE: Wiley-VCH, 2004.

[25] Y. J. Franzke and J. M. Yu, *J. Chem. Theory Comput.*, vol. 18, pp. 323–343, 2022.

[26] F. Bruder, Y. J. Franzke, and F. Weigend, *J. Phys. Chem. A*, vol. 126, pp. 5050–5069, 2022.

[27] S. Gillhuber, Y. J. Franzke, and F. Weigend, *J. Phys. Chem. A*, vol. 125, pp. 9707–9723, 2021.

[28] J. Autschbach, S. Patchkovskii, and B. Pritchard, *J. Chem. Theory Comput.*, vol. 7, pp. 2175–2188, 2011.

[29] K. Kundu, J. R. K. White, S. A. Moehring, J. M. Yu, *et al.*, *Nat. Chem.*, vol. 14, pp. 392–397, 2022.

[30] J.-D. Chai and M. Head-Gordon, *Phys. Chem. Chem. Phys.*, vol. 10, pp. 6615–6620, 2008.

[31] P. Jönsson, M. Godefroid, G. Gaigalas, J. Ekman, *et al.*, *Atoms*, vol. 11, pp. 1–44, 2023.

[32] C. F. Fischer, M. Godefroid, T. Brage, P. Jönsson, and G. Gaigalas, *J. Phys. B: At. Mol. Opt. Phys.*, vol. 49, p. 182 004, 2016.

[33] E. U. Condon and G. H. Shortley, *The Theory of Atomic Spectra*. Cambrigde, UK: Cambrigde University Press, 1935, pp. 79–111.

[34] M. P. Hehlen, M. G. Brik, and K. W. Krämer, *J. Lumin.*, vol. 136, pp. 221–239, 2013.

[35] A. Kramida, Y. Ralchenko, J.Reader, and N. A. Team, NIST Atomic Spectra Database (ver. 5.10). Available: `https://physics.nist.gov/asd` [May 31st, 2024]. National Institute of Standards and Technology, Gaithersburg, MD. 2022.

[36] M. Reiher and A. Wolf, *Relativistic Quantum Chemistry: The Fundamental Theory of Molecular Science*, Second edition. Weinheim, DE: WILEY-VCH Verlag, 2015.

[37] C. F. Fischer, G. Gaigalas, P. Jönsson, and J. Bieroń, *Comput. Phys. Commun.*, vol. 237, pp. 184–187, 2019.

[38] J. Bieroń, C. F. Fischer, G. Gaigalas, I. Grant, and P. Jönsson, A practical guide to Grasp2018. A collection of Fortran 95 programs with parallel computing using MPI.
Available: `https://github.com/compas/grasp/releases/tag/2018-12-03` [May 31st, 2024], 2018.

[39] L. Brillouin, *J. Phys. Radium*, vol. 3, pp. 373–389, 1932.

[40] G. Gaigalas and D. Kato, *Comput. Phys. Commun.*, vol. 261, p. 107 772, 2021.